Article

The Reactivity of Polyethylene Microplastics in Water under Low Oxygen Conditions Using Radiation Chemistry

Julie R. Peller [1,*], Stephen P. Mezyk [2], Sarah Shidler [3], Joe Castleman [1], Scott Kaiser [1] and Gregory P. Horne [4]

1   Department of Chemistry, 1710 Chapel Drive, Valparaiso University, Valparaiso, IN 46383, USA; joe.castleman@valpo.edu (J.C.); scott.kaiser@valpo.edu (S.K.)
2   Department of Chemistry, California State University, Long Beach, CA 90804, USA; Stephen.Mezyk@csulb.edu
3   Renishaw, Inc., West Dundee, IL 60118, USA; sarah.shidler@renishaw.com
4   Center for Radiation Chemistry Research, Idaho National Laboratory, P.O. Box 1625, Idaho Falls, ID 83415, USA; gregory.horne@inl.gov
*   Correspondence: julie.peller@valpo.edu

Abstract: Polyethylene (PE) is an intensely utilized polymer, which has consequently led to it becoming a common environmental contaminant. PE and other plastic waste are known to be highly persistent in surface waters; however, chemical and physical changes do take place over time, dependent mostly on highly variable natural conditions, such as oxygen (O_2) availability. Gamma radiation was used to generate reactive oxygen species, namely hydroxyl radicals, in initially aerated aqueous solutions to simulate the natural weathering of microplastics in waters where there are fluctuations and often depletions in dissolved O_2. The headspace of the irradiated PE-containing solutions was probed for the formation of degradation products using solid-phase microextraction (SPME) fibers in combination with gas chromatography mass spectrometry (GCMS). The major species detected were *n*-dodecane, with trace levels of tridecane, 2-dodecanone, and hexadecane, which were believed to be predominately adsorbed in the PE microplastics in excess of their aqueous solubility limits. Surface characterization by Raman spectroscopy and light and dark field microscopy indicated no change in the chemical composition of the irradiated PE microplastics under low O_2 to anaerobic conditions. However, morphological changes were observed, indicating radical combination reactions.

1. Introduction

Polyethylene (PE) is the most highly manufactured and utilized polymer in the world, with continuously projected growth as consumer demand in automobile, construction, packaging and other applications continues to rise [1,2]. In 2019, the global demand for PE was estimated at 47 million metric tons, due in part to broadened ethylene feedstock sources such as shale gas, coal, and bio-based materials [3]. PE is a highly recyclable plastic material since it has high thermal stability [4]. However, the rate of PE recycling was only 29.3% in 2018 in the United States (US) [5]. Plastic recycling rates vary around the globe, but the overall effective reuse of the material is minimal. The broader pool of polymer waste is mostly landfilled (~79%) or incinerated (12%) [6]. Another growing practice for waste PE and other olefin polymers is pyrolysis, which requires high temperatures (400–600 °C) to convert these polymers into smaller molecules for fuel or further processing [7–10].

A problematic outcome of the over nine billion metric tons of plastic generated since 1950 is a global environment containing a growing amount of persistent waste plastic [11]. Much of this waste contaminates surface waters, where it ultimately fragments into even more problematic microplastics [12]. A large pool of data has been published on the

presence of microplastics in the oceans [13,14], freshwater reservoirs [15,16], wetlands [17], sediments [18] and other environments [19]. PE is a commonly identified microplastic in water and other environmental media [20,21]. The distribution and fate of PE microplastics are dictated by a number of material factors, including size, shape, density and additives, and environmental conditions, such as temperature, pH, sunlight exposure, biofilms, wind and waves [22]. PE microplastics are expected to mostly subsist on water surfaces since their density is less than water—ranging from 0.86 g mL^{-1} for amorphous PE, to near 1.0 g mL^{-1} for crystalline PE [23].

Chemical transformations (weathering) of microplastics in the environment are initiated by factors such as light, heat, and/or reactions with reactive oxygen species and radicals—e.g., superoxide ($O_2^{\bullet-}$), hydroxyl radicals ($^\bullet OH$), singlet oxygen ($O^\bullet$), and/or ozone (O_3)—present in the environment. Highly implicated in the chemistry of materials in aqueous environments are the strongly oxidizing $^\bullet OH$ generated by the interaction of solar ultra-violet (UV) light and/or secondary chemical reactions, and typically present in a steady-state concentration range of 10^{-18} to 10^{-16} M in surface waters [24,25]. Additional radicals can also be created by UV light absorption by various water solutes, such as nitrate, nitrite, and dissolved organic matter, leading to additional reactive species capable of inducing chemical change in microplastics [26]. While many studies of microplastics' transformations have been conducted in the presence of consistent light and oxygen (O_2), much less is known about the weathering under reduced dissolved O_2 concentrations, especially their chemical reactivity, products released, and the lifetime of these particles. It is therefore important to explore the fate of microplastics under low O_2 to anaerobic conditions, where any radical-promoted chemical weathering would be followed by cross-linking and/or other reactions [27].

Radiation chemistry has been widely used to explore the stability of plastics and to manipulate polymeric materials [28–31]. Additionally, water radiolysis can be used to generate reactive oxygen species whose reactions simulate the natural weathering of microplastics [32,33]. Water radiolysis (Equation (1)) creates $^\bullet OH$ radicals (E° = 2.7 V) [34], one of the most powerful chemical oxidants according to: [32]

$$H_2O \rightsquigarrow [0.28]^\bullet OH + [0.06]H^\bullet + [0.27]e_{aq}^- + [0.05]H_2 + [0.07]H_2O_2 + [0.27]H_{aq}^+ \quad (1)$$
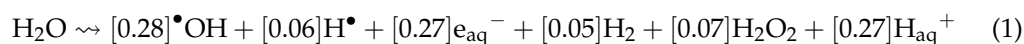
where the numbers in brackets in Equation (1) are the gamma radiolytic yields (μmol J^{-1}) of each produced species for neutral pH water. Further, dissolved O_2 is consumed by radiolytically generated reducing radicals from water radiolysis:
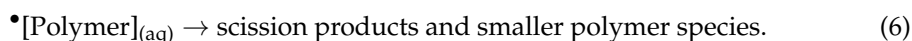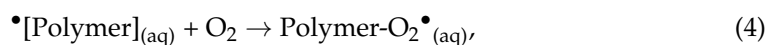
$$O_2 + e_{aq}^-/H^\bullet \rightarrow O_2^-/HO_2^\bullet \quad (2)$$

Cobalt-60 (^{60}Co) gamma radiation sources generate $^\bullet OH$ radicals at rates of 10^{-8} to 10^{-5} M s^{-1}, many orders of magnitude faster than experienced in real-world waters, which allows laboratory experiments to be conducted over short times to replicate long-term environmental weathering. In water, polymeric materials have been shown to undergo radical reactions, consistent with other carbon-based compounds [35]. Reactions with $^\bullet OH$ typically afford hydrogen–atom abstraction from polyolefins such as PE (Equation (3)), creating carbon-centered radicals ($^\bullet$[Polymer]):

$$^\bullet OH + Polymer_{(aq)} \rightarrow H_2O + {}^\bullet[Polymer]_{(aq)}. \quad (3)$$
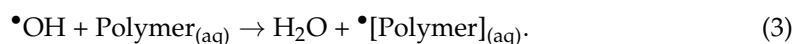
In aerated aqueous solutions (~0.25 mM O_2), carbon-centered radicals are expected to rapidly react with dissolved O_2 to form peroxyl radicals (Polymer-$O_2^\bullet$, Equation (4)), which can initiate polymer autooxidation through chain reactions. For the reactions of hydrocarbons in water under low O_2 to anaerobic conditions—potentially achieved by the radical consumption of O_2, (Equation (2))—the carbon-centered radical likely crosslinks with other carbon radicals (Equation (5)) or leads to scission products (Equation (6)) [36,37].

For example, Billamboz et al. reported the formation of unsaturated polymer segments from PE films submerged in water when O_2 was replaced by argon or nitrous oxide [37].

$$^\bullet[Polymer]_{(aq)} + O_2 \rightarrow Polymer\text{-}O_2{^\bullet}_{(aq)}, \tag{4}$$

$$^\bullet[Polymer]_{(aq)} + {^\bullet}[Polymer]_{(aq)} \rightarrow Polymer\text{-}Polymer_{(aq)}, \tag{5}$$

$$^\bullet[Polymer]_{(aq)} \rightarrow scission\ products\ and\ smaller\ polymer\ species. \tag{6}$$

To date, weathering studies of microplastics have simulated oxygenated conditions in surface waters, a critical aspect for understanding the behavior of these pollutants [38]. However, microplastics that encounter low O_2 to anaerobic conditions have not been thoroughly studied, yet these low O_2 concentration regimes exist in stagnant waters, lower water column areas, and transiently in all waters. These conditions may be part of the reason for prolonged lifetimes in the environment and lead to varying morphologies and products of microplastics, some of which may remain adsorbed [39]. Here, we present a radiation chemistry investigation into the radical-induced weathering of PE microplastics that experience fluctuations in dissolved O_2 concentrations by utilizing initially aerated water mixtures where dissolved O_2 is depleted over time by radical consumption (Equation (2)).

2. Materials and Methods

2.1. Chemicals

PE microplastics were purchased from MilliporeSigma (Burlington, MA, USA) with an average molecular weight (MW) of ~4000 g mol^{-1} and an average Mn~1700, as determined by gel permeation chromatography (GPC), and a density of 0.92 g/mL at 25 °C. Analytical standard grade *n*-dodecane (>99.8%), diisopropyl ether (anhydrous 99%), and sodium chloride (99.5% purity) were also sourced from MilliporeSigma. Laboratory water mixtures were prepared with Millipore MilliQ deionized water (18.2 MΩ). LCMS-grade acetonitrile and sodium tetraborate decahydrate, glycerol, and butyl alcohol, ≥99.5%, were purchased from MilliporeSigma and used for the ion chromatography solvent.

2.2. Lake Michigan Water

Lake water (pH 7.7) was collected from the southern shore of Lake Michigan and filtered using 0.22 μm nylon filter paper. The concentrations of the predominant anions, chloride (Cl^-), nitrate (NO_3^-) and sulfate (SO_4^{2-}), were determined using a Waters^{TM} (Waters Corporation, Milford, MA, USA) Liquid Chromatograph (LC) equipped with a Waters IC-Pak^{TM} anion column and conductivity detector. The LC solvent was a sodium borate/gluconate solution flowed at 1.0 mL min^{-1}.

2.3. Gamma Irradiations

PE water mixtures were irradiated using the Idaho National Laboratory (INL) Center for Radiation Chemistry (CR2) Foss Therapy Services Model 812 and the Notre Dame Radiation Laboratory (NDRL) Nordion Gammacell 220E ^{60}Co irradiators. Samples comprising ~100 mg of either original stock or purified PE neat were suspended in ~18 mL of DI water, saline solution simulant (0.5 M NaCl in Milli-Q water), or filtered Lake Michigan water sealed in 20 mL screw-cap scintillation vials. Samples were irradiated for a range of absorbed doses up to ~4 MGy and were considered anaerobic after ~4 kGy due to the radiolytic consumption of dissolved O_2. Dose rates for both ^{60}Co irradiators were determined by Fricke solution corrected for the radioactive decay of ^{60}Co ($\tau_{1/2}$ = 5.27 years), affording a range of 20–480 Gy min^{-1} [40].

2.4. Product Extractions and Material Analysis

Solid phase microextraction (SPME) was used to collect volatile and semi-volatile components of the irradiated water mixtures. Supelco^{TM} (Supelco, Inc., Bellefonte, PA, USA) 50/30 μm DVB/CAR/PDMS fibers were exposed to the headspace of the vials containing the PE–water mixtures for 30 min at 80–85 °C. The SPME fiber was then set in the injection

port of an Agilent (Agilent Technologies, Inc., Santa Clara, CA, USA) 7890A/5975C gas chromatography mass spectrometer (GCMS), where the collected compounds were released and then separated using an Agilent HP-5MS column (19091S-433UI, 30 m × 0.250 mm). After maintaining the column temperature at 50 °C for 5 min, it was ramped from 50 to 260 °C at 8°/min. The single quadrupole GC/MS generated the total ion chromatogram over the range of 50–500 at a scan speed of 3.2 scans/s. The MS source was set at 230 °C in positive ionization mode. Compounds were originally identified by GCMS using the National Institute of Science and Technology (NIST) database of compounds [41], followed by the purchase and testing of suspected compounds. The extracted compounds in the PE–water mixtures were then matched with the retention times and mass spectra of known compounds.

2.5. Adsorption Experiments

To determine the amounts of n-dodecane adsorbed to solid PE and partitioned in water, mixtures of PE microplastics (50 mg), water (10 mL) and n-dodecane (5 μL) were stirred for 24 h. Then, the solid PE microplastics were removed from the water using vacuum filtration. The n-dodecane adsorbed to the solid PE was extracted using diisopropyl ether (2 × 2 mL). Diisopropyl ether extractions were also performed on the solution water (2 × 2 mL). The extracts were run using a GCMS method using an autosampler (inlet temperature at 250 °C and column temperature ramped from 55 °C to 250 °C at 20 or 25 °C/min and the same MS conditions described above). The amount of n-dodecane in the diisopropyl ether extracts was quantified based on prepared solution standards.

2.6. Raman Spectroscopy

A Renishaw inVia Qontor confocal Raman microscope was used to analyze the PE samples. The inVia Qontor was equipped with a Leica DM2700 optical microscope with brightfield and darkfield microscopy capabilities. High spatial resolution Raman spectra were collected using 457 nm excitation, measuring 20 points/sample for 30 s/point using a 100× objective. A 2400 L/mm grating was used, capturing a spectral window from 379 to 2125 cm^{-1}. Prior to data collection, the instrument was calibrated using an internal Si sample, setting the first order silicon band to 520.5 cm^{-1}. All post processing, including baseline subtraction using an intelligent polynomial, normalization and curve fitting, were performed using the Renishaw WiRE software. Additionally, bulk measurements were made using a 20× objective with 457 nm excitation and the 2400 grating. A ten second extended scan over the spectral window from 100 cm^{-1} to 3500 cm^{-1} was collected for each sample for comparison of the fluorescence baseline.

3. Results and Discussion

3.1. Gamma Radiolysis of PE Microplastics in Water

Water mixtures containing the original commercial PE microplastics were found to contain numerous other chemicals, mostly volatile or semi-volatile hydrocarbons and ketones, as determined from SPME headspace extractions and GCMS analysis and shown in Figure 1 (red trace). Several mixtures of the original PE stock in water (Milli-Q) and salt water (0.5 M NaCl in Milli-Q) were prepared and subjected to gamma radiolysis. Beyond ~4 kGy of absorbed gamma dose, dissolved O$_2$ in the water was no longer present for chemical transformations. Therefore, since these PE stock microplastics were subjected to gamma doses between 0.5 and 2.0 MGy, O$_2$ was present only during the very early stages of these irradiations. A typical chromatogram for irradiated PE in water is also shown in Figure 1 (blue trace).
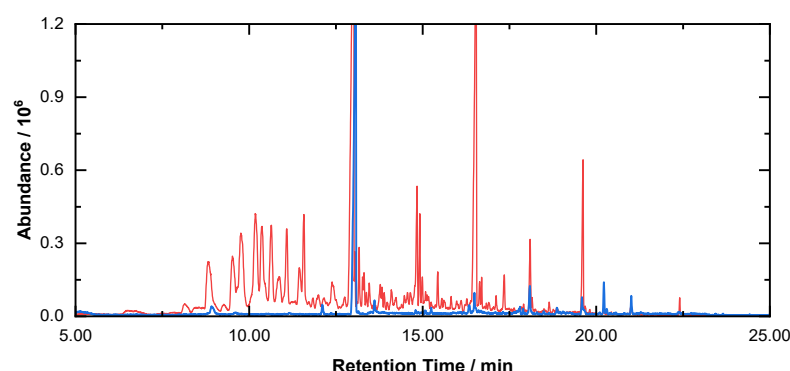
Figure 1. GCMS chromatograms of VOCs and sVOCs in the original PE stock (red) and after ~1 MGy gamma irradiation of original PE stock in water in a closed vessel (blue).

After irradiation, most of the identified contaminants from the original PE stock were no longer detectable. This is attributed to radicals from the radiolysis of water in the absence of O_2, namely $^\bullet OH$, hydrated electrons (e_{aq}^-), and hydrogen atoms ($H^\bullet$), having reacted to degrade these organic chemicals, similar to aqueous solutions containing dissolved organic contaminants [32]. However, a few of the original contaminants were still detected even after 2 MGy of absorbed dose, equivalent to >0.5 M $^\bullet OH$ radicals generated in situ. The most prominent compounds identified from the irradiated PE–water samples were *n*-dodecane, 2-dodecanone, and some other hydrocarbons listed in Table 1.

Table 1. Persistent compounds detected using the commercial PE stock in water or salt water after ~2 MGy of gamma irradiation.

Water	Salt Water
n-dodecane	*n*-dodecane
2-dodecanone	tridecane
	2-dodecanone
	hexadecane

For a few of the irradiated PE microplastic mixtures, the water was separated from the microplastics using vacuum filtration, and headspace extractions were performed on the water. No compounds were detected in the headspace of the separated water, indicating that the compounds collected in the headspace extractions were adsorbed to the PE. While no specific absorption data for these particular compounds have been reported for PE microplastics, previous studies measured significant adsorption (~6 g oil/g PE) of machine lubrication oil onto microplastics [42]. Other researchers found that the adsorption of both light and heavy crude oil fractions onto PE powders or sheets was enhanced when the PE had previously received 30 kGy of ^{60}Co irradiation [43].

To further investigate the presence of the most prevalent impurity, *n*-dodecane, in these irradiated aqueous PE samples, the removal of the chemical contaminants from the original PE stock was necessary. This was achieved by heating a thin layer of the solid PE microplastics in open air at 70 °C for at least 50 h. The blue trace chromatogram in Figure 2, (flat baseline), shows that the heat-treated PE stock no longer contains any significant levels of trace chemical contaminants, relative to the initial material (red trace). Based on the success of this simple purification/pre-treatment, all subsequent experiments utilized heat-treated PE, or purified PE.

Gamma irradiation experiments were then performed on the purified PE microplastics, in both Milli-Q and Milli-Q/0.50 M NaCl (saltwater) using similar radiation doses (~0.5–2 MGy) as the original PE stock. From the SPME headspace extractions of the irradiated, purified PE–water mixtures, only trace amounts of C_8–C_{12} hydrocarbons were extracted from a few samples. In approximately half of these analyzed samples, none of these hydrocarbon compounds were detected. This suggests that the reactions of PE microplastics with water radiolysis radicals at higher total absorbed gamma doses do

not lead to the formation of significant quantities of smaller molecules/PE degradation products. Similar results were obtained for experiments performed at lower dose rates for an absorbed gamma dose of approximately 25 kGy.
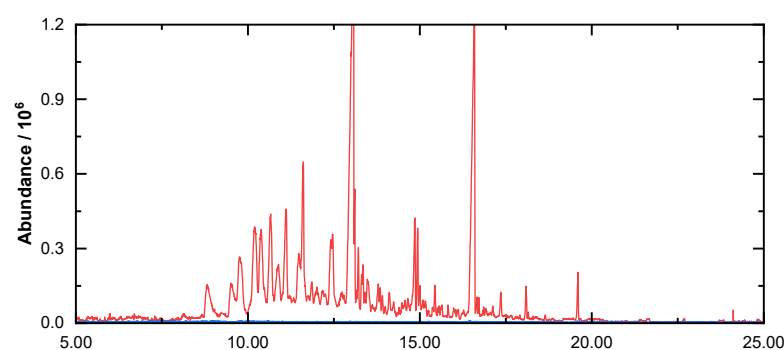

Figure 2. GCMS chromatogram of VOCs and sVOCs present in the commercial PE stock (red) and the absence of these compounds after 50 h of heating at 70 °C (blue).

Previous research has shown that small molecule scission products are preferentially formed when polymers in solution are irradiated at low dose rates, as this reduces the localized concentration of carbon-centered radicals, which in turn minimizes crosslinking reactions [44]. We investigated the effects of lower dose rates (20 Gy min^{-1}) and lower total irradiation doses on heat-treated PE microplastics in DI/Milli-Q water and simulated saltwater for low O_2 conditions. These low-dose samples were pre-saturated with nitrogen gas, and then subjected to 1 kGy of gamma irradiation, equivalent to ~280 μM •OH being generated in these aqueous solutions, far less than the equivalent amount of PE (100 mg) used in our 18 mL aqueous solutions. The products collected by SPME headspace extraction of mixtures irradiated to 1 kGy are listed in Table 2. The GCMS chromatograms (see Supplementary Information) for irradiated PE–water mixtures contained *n*-dodecane, 2-dodecanone, pentadecane, 2-tetradecanone, and 2-hexadecanone, of which *n*-dodecane was again the prominent product. Similar compounds were also identified in the complementary PE-salt water irradiations. These compounds, identified from the low irradiation dose PE–water mixtures, suggest that PE microplastics do undergo scission reactions to some extent in the absence of O_2. This contrasts with the reactivity of the PE microplastics exposed to higher radiation doses, which predominantly undergo crosslinking reactions.

Table 2. Compounds detected after gamma irradiation using heat-treated PE stock in Milli-Q water or salt water, or Lake Michigan (LM) water. (HCs = hydrocarbons).

~2 MGy or 25 kGy Water or Saltwater	~1 kGy Water Or Saltwater	~0.5 and 1.4 MGy LM Water	~2 MGy LM Water
trace amounts HCs	*n*-dodecane	*n*-dodecane	*n*-dodecane
	2-dodecanone	undecane	tridecane
	pentadecane		
	2-tetradecanone		
	2-hexadecanone		

To better simulate the behavior of PE microplastics in natural water conditions, Lake Michigan (LM, USA) water was used as a solvent for analogous purified PE gamma irradiation experiments. The lake water pH was 7.7, slightly higher than the laboratory deionized water pH of 7.2. The concentrations of chloride, sulfate and nitrate were determined to be 12, 23 and 0.7 ppm, respectively. The typical dissolved organic carbon content of lake water is around 2 ppm [45]. Here, *n*-dodecane was again the only detected compound in the samples that were subjected to doses of ~0.5 and 1.4 MGy. A smaller amount of *n*-dodecane and additional hydrocarbons (e.g., undecane and tridecane) were detected in samples irradiated to ~2.0 MGy. A few scission products were also formed at these high

doses when the lake water was the solvent, in contrast to the irradiated pure water and saltwater solutions, as shown in Table 2.

3.2. Adsorption Experiments of Dodecane with PE

In the irradiated, original PE stock, the major compound that was formed during radiolysis and/or seemingly eluded radical-induced degradation reactions was *n*-dodecane. The very low water solubility of *n*-dodecane (3.7 mg L^{-1} at room temperature) [46] and absence of tertiary carbons that stabilize radicals may account for part of its aqueous radiation stability. A standard aqueous solution of *n*-dodecane at its saturation concentration was tested using the SPME headspace method. While the SPME method is considered only semi-quantitative [47], the integrated area from the subsequent GCMS analysis was significantly lower than the areas detected from the headspace analysis of the irradiated PE–water mixtures.

The wide variation in the amount of *n*-dodecane extracted from the different PE–water mixtures and the standard aqueous *n*-dodecane solution, which did not contain any PE, is shown in Figure 3. These data suggest that *n*-dodecane adsorbs strongly to PE, enabling its presence in the water mixture well beyond its water solubility limit. Further, through adsorption, *n*-dodecane potentially evades the expected radical-induced solution chemistry. Our data also indicate that *n*-dodecane is a product of the radical-induced degradation of PE. The size of the scission products is consistent with previous experiments for the direct exposure of PE–water mixtures to UV light and O$_2$, which promoted the formation of dicarboxylic acids of C$_8$–C$_{12}$ chain lengths and dissolved organic carbon [48,49]. Overall, the radical-induced degradation (weathering) of PE microplastics in water is slower than other polymers that contain tertiary carbons, which are more subject to radical transformations owing to the stabilization of radical centers by hyperconjugation [50].
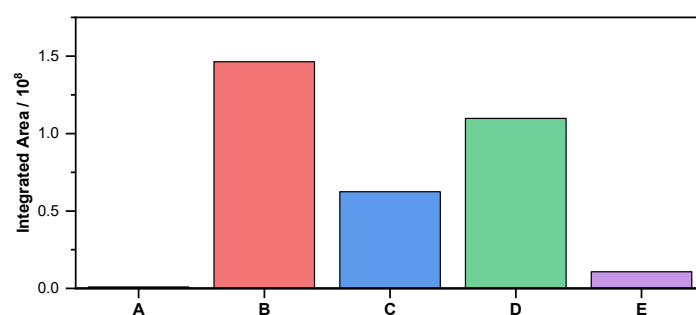

Figure 3. Integrated areas from GCMS peaks for *n*-dodecane extracted (SPME) from: (**A**) 3.7 ppm dodecane in water; (**B**) original PE in water, ~0.5 MGy; (**C**) original PE in water, ~2 MGy; (**D**) original PE in saltwater, ~0.5 MGy; (**E**) original PE in water, no irradiation. The vertical axis represents 10^9 integration values.

The interactions between PE, *n*-dodecane and water were further probed quantitatively using *n*-dodecane well above its water solubility. In each case, no *n*-dodecane was detected in the water. Most of the 22 µmols of *n*-dodecane was recovered from the subsequent extractions of PE with diisopropyl ether, indicating that *n*-dodecane adsorbs strongly to PE microplastics. Given that studies of weathered PE, which contain adsorbed chemicals, show that endocrine disruption effects in adult fish are higher than with pure PE [51], these types of investigations are important for predicting the toxic nature of PE in natural water environments. Our studies indicate that when *n*-dodecane forms as a scission product from the gamma radiolysis of PE, it remains adsorbed to the surface of the PE microplastic particle.

3.3. Raman Analysis of Irradiated PE

To assess radical-induced surfaces changes of the PE microplastics, analyses were conducted using Raman spectroscopy and bright field and dark field microscopy. When the irradiated PE microplastics were viewed under the stereomicroscope at 45× magnification,

many particles appeared to have crosslinked. Figure 4 shows representative examples of PE microplastics before and after solution gamma irradiation. Magnified PE particles observed under dark field microscopy for irradiations of 0.5–2.0 MGy suggest induced surface divets and/or crosslinked particles.
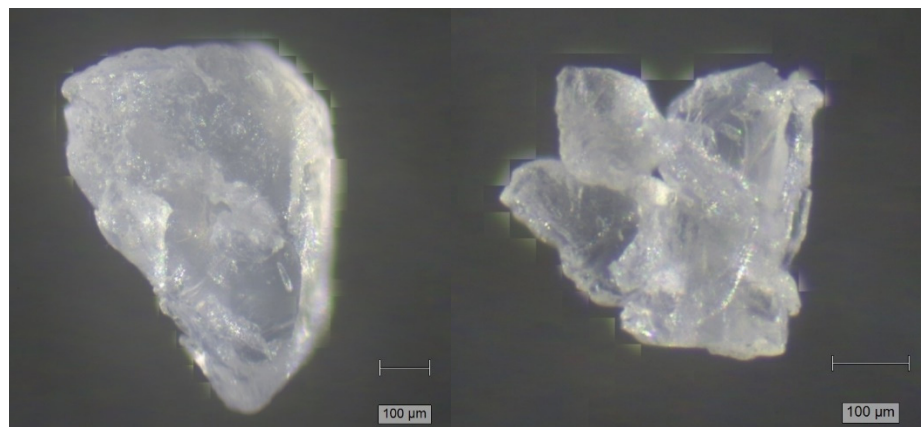

Figure 4. PE microplastic particles viewed using dark field microscopy. The left image is a non-irradiated PE particle, and the right image is post-high-dose irradiation.

Figure 5 shows representative Raman spectra for non-irradiated PE (black trace) and irradiated PE samples. The Raman signals, exemplifying chemical structures, are essentially the same for all of the samples. Further examination of the extended scan of the Raman fingerprint region out to the CH stretch bands indicates an increase in the fluorescence background for the irradiated PE samples. Such a fluorescence increase can indicate the formation of defects or other impurities on the PE surface. However, no impurities were identified. The absence of data showing chemical changes of the hydrocarbon backbone suggests that PE microplastics will persist, and possibly combine to form larger particles when in contact with other microplastics in low O_2 to anaerobic aqueous environments. These data support the expected reactivity in Equations (3) and (5), crosslinking and fragmentation, predicted to primarily occur under the low O_2 conditions.
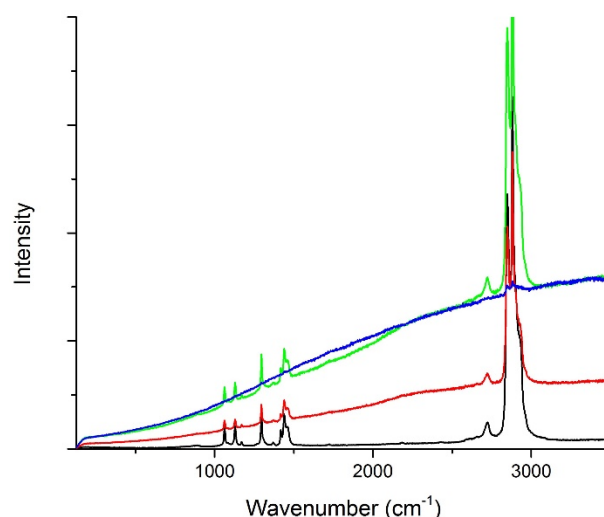

Figure 5. Raman spectra using 475 nm excitation of gamma-irradiated PE in fresh water (red trace), salt water (green trace), and Lake Michigan water (blue trace) show substantial fluorescence in comparison to the stock PE (black trace).

For each irradiated PE sample, high spatial resolution data were collected using a $100\times$ objective, with an estimated sampling depth of 1.3 μm, from twenty locations on a single particle. The CH_2 twisting band intensity at 1296 cm^{-1} was used to normalize

each spectrum for comparison. Typical spectra are shown in Figure 6 and additional spectra are included in the Supplementary Information. Analysis of the CH_2 bending and twisting bands can be used to calculate the fractions of amorphous and crystalline phases. Crystalline-phase PE contributes to the CH_2 bending band at 1416 cm^{-1} while the amorphous phase is indicated by a CH_2 bending band at 1440 cm^{-1} and a shoulder on the CH_2 twisting band at 1303 cm^{-1} [52]. Minimal changes were seen in the calculated fraction for the amorphous phase, suggesting that at these radiation doses in water media, the PE does not undergo any significant structural changes. This is consistent with the SPME headspace extraction results which did not find the formation of smaller molecules or PE degradation products at the total absorbed doses between 0.5–2.0 MGy.
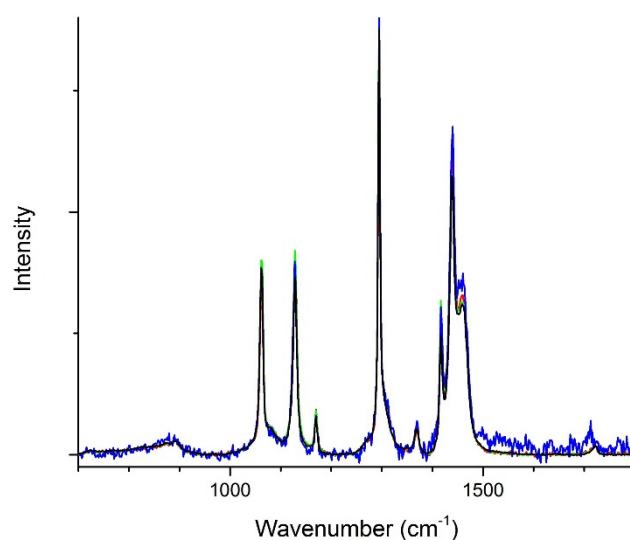

Figure 6. Baseline subtracted high-resolution Raman spectra showing the C-C stretch, CH_2 twisting and CH_2 bending bands of gamma irradiated PE in fresh water (red trace), salt water (green trace), and Lake Michigan water (blue trace) showing minimal changes in comparison to the stock PE (black trace).

4. Conclusions

The irradiation of PE microplastics in aqueous environments under low O_2 to anaerobic conditions showed that the radical-induced processes yielded a variety of aliphatic hydrocarbon scission degradation products. Of these, *n*-dodecane was dominant, and found in significant excess of its aqueous solubility limit owing to adsorption on the surface of the PE microplastics. Such adsorption of hydrophobic degradation products to these surfaces may provide a real-world weathering protection mechanism, whereby radicals preferentially react with these adsorbed compounds as opposed to the polymer itself, thereby prolonging the environmental lifetime of the PE microplastic.

This scenario is supported by the absence of significant chemical and structural changes in the irradiated PE microplastics, as investigated by Raman spectroscopy. Evidence of crosslinking suggests that the current weathering paradigm of macropolymers undergoing successive degradation into smaller polymer fragments is not entirely correct, especially when O_2 is limited. In contrast, aerated, aqueous conditions lead to oxidized surfaces and products [53,54].

Overall, the presented findings suggest that currently anticipated microplastic lifetimes in the environment could be severely underestimated, especially for stagnant waters and lower water column areas. Further studies are currently underway to elucidate the role of O_2 in these PE microplastic aqueous systems, in order to establish a holistic description for radical-induced weathering of microplastic in world waters.

Supplementary Materials: The following are available online at https://www.mdpi.com/article/10.3390/w13213120/s1, Figure S1. Standard graph of dodecane [mM] in diisopropyl ether. Figure S2.

PE (as received) in salt water (0.5 M), irradiation dose of ~0.5 MGy. Figure S3. PE (as received) in water, irradiation dose of ~1.5 MGy. Largest peak is *n*-dodecane. Figure S4. PE (heat-treated) in Lake Michigan water, irradiation dose of ~0.5 MGy. Largest peak is *n*-dodecane. Figure S5. PE (heat-treated) in salt water, irradiation dose of ~2.0 MGy. No detectable compounds. Figure S6. Chromatogram of *n*-dodecane (3.8 mg/L, maximum solubility) in water without PE present. Compiled data are shown in Figure 3. The integrated area is 954,018. Figure S7. Chromatogram of *n*-dodecane in a saltwater mixture containing "as received" PE iradiated for ~0.5 MGy. Compiled data are shown in Figure 3. The integrated area is 54,198,238. Figure S8. Chromatogram of *n*-dodecane in a water mixture containing "as received" PE iradiated for ~2.0 MGy. Compiled data are shown in Figure 3. The integrated area is 62,442,370. Figure S9. Baseline subtracted high resolution Raman spectra showing the CH_2 twisting, and CH_2 bending bands of gamma irradiated PE in fresh water (red trace), salt water (green trace), and Lake Michigan water (blue trace) showing minimal changes in comparison to the stock PE (black trace). Raman bands indicative of crystalline phase PE are highlighted in grey and bands indicating amorphous phase PE are highlighted in yellow. Table S1. Identified Peaks from Figure S2, determined using purchased standards.

References

1. ARC, I. *Polyethylene Market—Forecast(2021–2026)*; CMR 0514; Furion analystic Research &Consulting LLP: Hyderabad, India, 2021.
2. Ahuja, K.; Mamtani, K. *Automotive Plastics Market Size, Share and Industry Analysis Report by Product (Polyurethane, PVC, Polyethylene, Polypropylene, ABS, Polycarbonate, Polyamide, PMMA) and Application (Electrical Components, Power Train, Under the Hood, Chassis, Interior & Exterior Furnishings), Regional Outlook, Application Potentail, Competitive Market Share & Forecast, 2017–2024*; Global Market Insights, Inc.: Selbyville, DE, USA, 2018.
3. Tiseo, I. *Global Polyethylene Demand and Capacity 2015–2022*; Statista: Hamburg, Germany, 2021.
4. Cho, K.C.; Lee, B.H.; Hwang, K.M.; Lee, H.S.; Choe, S.J. Rheological and mechanical properties in polyethylene blends. *Polym. Eng. Sci.* **1998**, *38*, 1969–1975. [CrossRef]
5. United States Environmental Protection Agency. Plastics: Material-Specific Data. 2020. Available online: https://www.epa.gov/facts-and-figures-about-materials-waste-and-recycling/plastics-material-specific-data (accessed on 28 August 2021).
6. Geyer, R.; Jambeck, J.R.; Lavendar Law, K. Production, use, and fate of all plastics ever made. *Sci. Adv.* **2017**, *3*, e1700782. [CrossRef] [PubMed]
7. Costa, P.A.; Pinto, F.J.; Ramos, A.M.; Gulyurtlu, I.K.; Cabrita, I.A.; Bernardo, M.S. Kinetic evaluation of the pyrolysis of polyethylene waste. *Energy Fuels* **2007**, *21*, 2489–2498. [CrossRef]
8. Peterson, J.D.; Vyazovkin, S.; Wight, C.A. Kinetics of the thermal and thermo-oxidative degradation of polystyrene, polyethylene and poly(propylene). *Macromol. Chem. Phys.* **2001**, *202*, 775–784. [CrossRef]
9. Sharuddin, S.D.A.; Abnisa, F.; Daud, W.; Aroua, M.K. A review on pyrolysis of plastic wastes. *Energy Conv. Manag.* **2016**, *115*, 308–326. [CrossRef]
10. Britt, P.F. *Report of the Basic Energy Sciences Roundtable on Chemical Upcycling of Polymers*; U.S. Department of Energy Office of Science: Washington, DC, USA, 2019.
11. Tiseo, I. Global Plastics Industry—Statistics & Facts. Available online: https://www.statista.com/topics/5266/plastics-industry/ (accessed on 28 August 2021).

12. Rahimi, A.; Garcia, J.M. Chemical recycling of waste plastics for new materials production. *Nat. Rev. Chem.* **2017**, *1*, 11. [CrossRef]
13. Kane, I.A.; Clare, M.A. Dispersion, Accumulation, and the Ultimate Fate of Microplastics in Deep-Marine Environments: A Review and Future Directions. *Front. Earth Sci.* **2019**, *7*, 27. [CrossRef]
14. GSAMP. *Sources, Fate and Effects of Microplastics in the Marine Environment: A Global Assessment*; Joint Group of Experts on the Scientific Aspects of Marine Environmental Protection: London, UK, 2015.
15. Peller, J.R.; Nelson, C.; Iceman, C.; Kostelnik, E.; Ganesh Babu, B. A review of microplastics in freshwater environments: Locations, methods and pollution loads. In *Current Status of Environmental Research on Water Contaminants*; Ahuja, S., Ed.; ACS Books: Washington, DC, USA, 2020.
16. Jiang, C.B.; Yin, L.S.; Li, Z.W.; Wen, X.F.; Luo, X.; Hu, S.P.; Yang, H.Y.; Long, Y.N.; Deng, B.; Huang, L.Z.; et al. Microplastic pollution in the rivers of the Tibet Plateau. *Environ. Pollut.* **2019**, *249*, 91–98. [CrossRef] [PubMed]
17. Qian, J.; Tang, S.J.; Wang, P.F.; Lu, B.H.; Li, K.; Jin, W.; He, X.X. From source to sink: Review and prospects of microplastics in wetland ecosystems. *Sci. Total Environ.* **2021**, *758*, 17. [CrossRef]
18. Peller, J.R.; McCool, J.P.; Watters, M. Microplastics in Soils and Sediment: Sources, Methodologies, and Interactions with Microorganisms. In *Handbook of Microplastics in the Environment*; Rocha-Santos, T., Costa, M., Mouneyrac, C., Eds.; Springer Nature Switzerland: Cham, Switzerland, 2020.
19. Peller, J.; Nevers, M.B.; Byappanahalli, M.; Nelson, C.; Babu, B.G.; Evans, M.A.; Kostelnik, E.; Keller, M.; Johnston, J.; Shidler, S. Sequestration of microfibers and other microplastics by green algae, Cladophora, in the US Great Lakes. *Environ. Pollut.* **2021**, *276*, 116695. [CrossRef]
20. Li, C.R.; Busquets, R.; Campos, L.C. Assessment of microplastics in freshwater systems: A review. *Sci. Total Environ.* **2020**, *707*, 12. [CrossRef]
21. Lebreton, L.; Slat, B.; Ferrari, F.; Sainte-Rose, B.; Aitken, J.; Marthouse, R.; Hajbane, S.; Cunsolo, S.; Schwarz, A.; Levivier, A.; et al. Evidence that the Great Pacific Garbage Patch is rapidly accumulating plastic. *Sci. Rep.* **2018**, *8*, 15. [CrossRef]
22. Duan, J.J.; Bolan, N.; Li, Y.; Ding, S.Y.; Atugoda, T.; Vithanage, M.; Sarkar, B.; Tsang, D.C.W.; Kirkham, M.B. Weathering of microplastics and interaction with other coexisting constituents in terrestrial and aquatic environments. *Water Res.* **2021**, *196*, 16. [CrossRef]
23. Moy, F.H.; Kamal, M.R. Crystalline and amorphous orientations in injection molded polyethylene. *Polym. Eng. Sci.* **1980**, *20*, 957–964. [CrossRef]
24. Santoke, H.; Cooper, W.J. Environmental photochemical fate of selected pharmaceutical compounds in natural and reconstituted Suwannee River water: Role of reactive species in indirect photolysis. *Sci. Total Environ.* **2017**, *580*, 626–631. [CrossRef]
25. Zhou, X.L.; Mopper, K. Determination of photochemically produced hydroxyl radicals in seawater and fresh-water. *Mar. Chem.* **1990**, *30*, 71–88. [CrossRef]
26. Calza, P.; Vione, D.; Novelli, A.; Pelizzetti, E.; Minero, C. The role of nitrite and nitrate ions as photosensitizers in the phototransformation of phenolic compounds in seawater. *Sci. Total Environ.* **2012**, *439*, 67–75. [CrossRef] [PubMed]
27. Grause, G.; Chien, M.F.; Inoue, C. Changes during the weathering of polyolefins. *Polym. Degrad. Stab.* **2020**, *181*, 21. [CrossRef]
28. Burillo, G.; Clough, R.L.; Czvikovszky, T.; Guven, O.; Le Moel, A.; Liu, W.W.; Singh, A.; Yang, J.T.; Zaharescu, T. Polymer recycling: Potential application of radiation technology. *Radiat. Phys. Chem.* **2002**, *64*, 41–51. [CrossRef]
29. Negrin, M.; Macerata, E.; Consolati, G.; Quasso, F.; Lucotti, A.; Tommasini, M.; Genovese, L.; Soccio, M.; Lotti, N.; Mariani, M. Effect of Gamma Irradiation on Fully Aliphatic Poly(Propylene/Neopentyl Cyclohexanedicarboxylate) Random Copolymers. *J. Polym. Environ.* **2018**, *26*, 3017–3033. [CrossRef]
30. Gulmine, J.V.; Akcelrud, L. FTIR characterization of aged XLPE. *Polym. Test* **2006**, *25*, 932–942. [CrossRef]
31. Ferry, M.; Ngono, Y. Energy transfer in polymers submitted to ionizing radiation: A review. *Radiat. Phys. Chem.* **2021**, *180*, 109320. [CrossRef]
32. Buxton, G.; Greenstock, C.; Helman, W.P.; Ross, A.B. Critical Review of Rate Constants for Reactions of Hydrated Electrons, Hydrogen Atoms and Hydroxyl Radicals (OH/O$^-$) in Aqueous Solution. *J. Phys. Chem. Ref. Data* **1988**, *17*, 513–886. [CrossRef]
33. Spinks, J.W.T.; Woods, R.J. *An Introduction to Radiation Chemistry*; John Wiley & Sons: New York, NY, USA, 1990.
34. Ulanski, P.; Bothe, E.; von Sonntag, C. OH radical induced depolymerization of poly(methacrylic acid). *Nucl. Instrum. Methods Phys. Res. Sect. B-Beam Interact. Mater. Atoms* **1999**, *151*, 350–355. [CrossRef]
35. ter Halle, A.; Ladirat, L.; Martignac, M.; Mingotaud, A.F.; Boyron, O.; Perez, E. To what extent are microplastics from the open ocean weathered? *Environ. Pollut.* **2017**, *227*, 167–174. [CrossRef] [PubMed]
36. Getoff, N. Radiation-Degradation and photoinduced-degradation of pollutants in water—A comparative study. *Radiat. Phys. Chem.* **1991**, *37*, 673–680. [CrossRef]
37. Billamboz, N.; Grivet, M.; Foley, S.; Baldacchino, G.; Hubinois, J.C. Radiolysis of the polyethylene/water system: Studies on the role of hydroxyl radical. *Radiat. Phys. Chem.* **2010**, *79*, 36–40. [CrossRef]
38. Alimi, O.S.; Claveau-Mallet, D.; Kurusu, R.S.; Lapointe, M.; Bayen, S.; Tufenkji, N. Weathering pathways and protocols for environmentally relevant microplastics and nanoplastics: What are we missing? *J. Hazard. Mater.* **2022**, *423*, 126955. [CrossRef] [PubMed]
39. Binda, G.; Spanu, D.; Monticelli, D.; Pozzi, A.; Bellasi, A.; Bettinetti, R.; Carnati, S.; Nizzetto, L. Unfolding the interaction between microplastics and (trace) elements in water: A critical review. *Water Res.* **2021**, *204*, 117637. [CrossRef]

40. Fricke, H.; Hart, E.J. Studies of Reactions Induced by the Photoactivation of the Water Molecule. I. *J. Chem. Phys.* **1936**, *4*, 418–422. [CrossRef]

41. NIST/EPA/NIH Mass Spectral Library (EI). *National Institute of Standards and Technology*; Department of Commerce: Gaithersburg, MD, USA, 2018.

42. Hu, J.; Yang, S.; Guo, L.; Xu, X.Q.; Yao, T.; Xie, F. Microscopic investigation on the adsorption of lucrication oil on microplastics. *J. Mol. Liq.* **2017**, *227*, 351–355. [CrossRef]

43. Aboul-Gheit, A.K.; Khalil, F.H.; Abdel-Moghny, T. Adsorption of spilled oil from seawater by waste plastic. *Oil Gas Sci. Technol. -Rev. D Ifp. Energ. Nouv.* **2006**, *61*, 259–268. [CrossRef]

44. Miller, A.A.; Lawton, E.J.; Balwit, J.S. Effect of chemical structure of vinyl polymers on crosslinking and degradation by ionizing radiation. *J. Polym. Sci.* **1954**, *14*, 503–504. [CrossRef]

45. Laird, G.A.; Scavia, D. Distribution of labile dissolved organic-carbon in Lake Michigan. *Limnol. Oceanogr.* **1990**, *35*, 443–447. [CrossRef]

46. Hefter, G.T. (Ed.) *Hydrocarbons with Water and Seawater*; Pergamon Press: Oxford, UK, 1989; Volume 38, p. 582.

47. Kotowska, U.; Zalikowski, M.; Isidorov, V.A. HS-SPME/GC-MS analysis of volatile and semi-volatile organic compounds emitted from municipal sewage sludge. *Environ. Monit. Assess.* **2012**, *184*, 2893–2907. [CrossRef] [PubMed]

48. Gewert, B.; Plassmann, M.; Sandblom, O.; MacLeod, M. Identification of Chain Scission Products Released to Water by Plastic Exposed to Ultraviolet Light. *Environ. Sci. Technol. Lett.* **2018**, *5*, 272–276. [CrossRef]

49. Zhu, L.X.; Zhao, S.Y.; Bittar, T.B.; Stubbins, M.; Li, D.J. Photochemical dissolution of buoyant microplastics to dissolved organic carbon: Rates and microbial impacts. *J. Hazard. Mater.* **2020**, *383*, 10. [CrossRef]

50. Gewert, B.; Plassmann, M.M.; MacLeod, M. Pathways for degradation of plastic polymers floating in the marine environment. *Environ. Sci.-Process Impacts* **2015**, *17*, 1513–1521. [CrossRef] [PubMed]

51. Rochman, C.M.; Kurobe, T.; Flores, I.; Teh, S.J. Early warning signs of endocrine disruption in adult fish from the ingestion of polyethylene with and without sorbed chemical pollutants from the marine environment. *Sci. Total Environ.* **2014**, *493*, 656–661. [CrossRef]

52. Lin, W.; Cossar, M.; Dang, V.; Teh, J. The application of Raman spectroscopy to three-phase characterization of polyethylene crystallinity. *Polym. Test.* **2007**, *26*, 814–821. [CrossRef]

53. Dong, M.T.; Zhang, Q.Q.; Xing, X.L.; Chen, W.; She, Z.B.; Luo, Z.J. Raman spectra and surface changes of microplastics weathered under natural environments. *Sci. Total Environ.* **2020**, *739*, 139990. [CrossRef] [PubMed]

54. Liu, P.; Qian, L.; Wang, H.Y.; Zhan, X.; Lu, K.; Gu, C.; Gao, S.X. New Insights into the Aging Behavior of Microplastics Accelerated by Advanced Oxidation Processes. *Environ. Sci. Technol.* **2019**, *53*, 3579–3588. [CrossRef] [PubMed]